Pair interaction energies and local structures of titanium and nickel atom-pairs in β-Sn type silicon

Pair Interaction Energies and Local Structures of Titanium and Nickel Atom-pairs in β-Sn type Silicon

Nobuhisa Fujima[a,*], Taku Murakami[a], Toshiharu Hoshino[a], Mikio Fukuhara[b]

[a] *Dep. Electronics and Material Science, Shizuoka University, Hamamatsu Japan*
[b] *New Industry Creation Hatchery Center, Tohoku University, Sendai, Japan*

Abstract

Pair interaction energies (PIEs) of Ti-Ti, Ti-Ni and Ni-Ni pairs and optimized local structures around these pairs in β-Sn type Si are studied by first principles calculation to elucidate typical local structures of transition-metal (TM) atoms in Si-rich amorphous silicides or alloys. In the calculations, TM pairs are located at substitutional sites along a long axis of cuboid $Si_{432}(TM_2Si_{430})$ supercell (6×3×6 unit cells of β-Sn type Si) to calculate interatomic distance dependences of PIEs up to 6Å-distance (up to the 12th nearest neighboring (NN) distance). We find that interatomic distances of Ti-Ti and Ti-Ni pairs with largely negative PIEs agree with those in Si-rich ordered silicides such as $TiSi_2$ and $Ti_4Ni_4Si_7$, and that the optimized local structures around Ti-Ti and Ti-Ni pairs commonly have Si-hexagons, which typically appear in early-TM silicides, and thus expected to be observed in the amorphous Si-rich silicides or alloys. On the contrary, Ni-Ni pair in β-Sn type Si indicates no significant feature in PIE profile or in local structures. Properties of Ni-Ni or Ni-Si bonding in Si-rich silicides may be governed by sp^3-like Si lattices.

Keywords: Pair Interaction Energy, Transition-Metal Silicide, Amorphous alloys, Computer Simulations

1. Introduction

Transition-metal (TM) silicide has been widely studied as spintronics and thermoelectric materials. Recently not only ordered but also amorphous TM silicides have been investigated to develop new semiconducting materials, especially for junction or anode of semiconductor device. For example, Ma has reported amorphous Ti silicides with Ti-composition of 35-65 at% formed around interfaces of Ti-Si thin-film multilayers[1]. Okada et al. realized a low barrier and low resistance electrical junction by amorphous W-silicide with the typical local structure of WSi_n(n = 8-11)[2, 3]. They have also investigated amorphous TM silicides composed of the local structure of $TMSi_n$ (TM=Zr, Nb or Mo, n = 7-20), which have an optical gap (>0.4 eV) and large electron and hole mobilities[4]. Moreover, Fukuhara et al. proposed a super capacitor fabricated by dealloying amorphous ternary Ti-Ni-Si alloy followed by anodic oxidization, where nanoporous titanium oxides are formed[5, 6]. A Si-Ti-Ni alloy based on $Ti_4Ni_4Si_7$ matrix also has been investigated as an anode for all-solid-state Li-ion battery[7]. To achieve required performance in applications and to explore newly functional materials, it is very important to elucidate local structures of these amorphous silicides, where typical (but not rigidly fixed) structures are expected to be observed.

Zhang et al. reported atomic and electronic structures of 3d-TM single atoms (V-Ni) as a dopant in diamond type Si on the basis of first principles calculation[8]. They found, by comparing the formation energy of different dopant sites, that these 3d-TM atoms are energetically favorably located at the tetrahedral interstitial site in the diamond-Si lattice (actually at the hexagonal site only for Ni atom with the almost same energy as the tetrahedral site). Similar results of the preferred atomic site for single Ti and Ni atom in the diamond type Si have been obtained theoretically by Kamon et al[9]. Their results give a fundamental knowledge of TM atoms as dopants in diamond type Si.

However, structures of TM-silicides, even for Si-rich one, are not always based on the sp^3-like diamond structure. Then to discuss structures and properties of TM-silicides or alloys, especially local structures in amorphous alloys, we have to elucidate the interactions between TM atoms and those between TM-Si atoms in non-diamond type Si.

There are several slightly complicated structures in Si-rich Si-TM alloys, while we can recognize some common structures among these. For example, structures of late-TM disilicides, $CoSi_2$ and $NiSi_2$ are CaF_2-type(cF12), where a Si atom connects with four Co/Ni atoms as the sp^3-like manner, that is, they constitute a regular tetrahedron. On the other hand, early-TM disilicides, $TiSi_2$(C54:oF24), VSi_2(hP9) and $CrSi_2$(hP9) have Si-hexagons in-plane, where a Ti/V/Cr atom is located at the center of Si-hexagon, which suggest sp^2-like Si bonds. These typical Si struc-

*Corresponding author
Email address: fujima.nobuhisa@shizuoka.ac.jp (Nobuhisa Fujima)

tures of course should appear in such ordered compounds. However, these are also expected to appear as locally stable (metastable) partial structures in amorphous or disordered Si-rich compounds.

In the present paper, we calculate pair interaction energy (PIE) of Ti-Ti, Ti-Ni and Ni-Ni pairs in β-Sn type Si by first principle calculation to discuss energetically favorable site of the impurity-pair and the local atomic structures around the pairs. PIE indicates the energy deference between impurity pairs which are located at relatively different positions in a host material. A largely negative PIE means that the pair is energetically preferred to be at the position, and give a relatively stable structure around the pair under the precondition of dissolution of impurities in the host material. Therefore, PIE with structural relaxation is considered to be one of suitable tool to discuss the local structure of minority elements in both ordered and disordered host materials. We have studied atomic structures of Al-rich Al-TM alloys by using TM-TM PIEs in fcc Al calculated by the full-potential Korringa-Kohn-Rostoker Greens function method, and clarified the origins of the $L1_2$ and DO_{22} structures of Al_3Sc and Al_3V, etc[10, 11]. For Ni-rich Ni-Si alloys, effective pair interaction energies of Ni-Si in fcc-Ni have been calculated by using short-range order parameters[12].

Titanium and Nickel are selected here as a representative of early- and late-3d element of TM silicides, respectively. Although not the ground state of Si under atmospheric pressure, we employ the β-Sn type structure as a host lattice because the coordination number or density is more suitable for silicides than that in diamond type Si.

We find that Ti-Ti interatomic distances in the relaxed local structures with low PIEs almost agree with those in ordered Si-rich Si-Ti or Si-Ti-Ni alloys and that some common local structures appear around a Ti atom or the Ti-Ti pair. We also find that a similar situation to Ti-Ti PIEs appears in Ti-Ni PIEs. However, it is found that all the Ni-Ni PIEs in β-Sn type Si are positive and give no information about the energetically favorable structure. Instead, we show that the optimized Ni-Ni interatomic distances with low PIEs in the diamond type Si agree with the Ni-Ni interatomic distances in ordered Si-rich Ni silicides. The optimized Ni-Ni interatomic distances almost correspond with the Si-Si interatomic distances in the diamond type structure.

2. Calculations

We calculate PIE of Ti-Ti, Ti-Ni and Ni-Ni on substitutional sites in β-Sn type Si crystal (A5,tI4) with full structural optimization. TM-TM PIE with structural optimization, $\Delta E_{\rm opt}^{\rm TM\text{-}TM}$ is defined as a total energy difference between a optimized system with two TM atoms with a distance R, $E_{\rm opt}^{\rm TM\text{-}TM}(R)$, and that with the infinitely separated (non-interacting) two TM atoms, $E_{\rm opt}^{\rm TM\text{-}TM}(\infty)$ (here TM-TM=Ti-Ti, Ti-Ni or Ni-Ni):

$$\Delta E_{\rm opt}^{\rm TM\text{-}TM}(R) = E_{\rm opt}^{\rm TM\text{-}TM}(R) - E_{\rm opt}^{\rm TM\text{-}TM}(\infty). \quad (1)$$

We employ 432-atom supercell (2×216-atom cuboid: 28.14×14.07× for the two-impurity system (TM_2Si_{430}), and $E_{\rm opt}^{\rm TM\text{-}TM}(\infty)$ is approximated by the total energy $E_{\rm opt}^{\rm TM\text{-}TM}(R = 14.07\text{Å})$. The TM-TM distance R is taken along the long axis (a-axis) of the supercell. We calculate PIEs from the 1st nearest neighboring(NN) pair (initial distance of 2.43 Å) to the 12th NN pair (initial distance of 5.59 Å) in the supercell.

In the β-Sn type Si, Si atoms align in a zigzag along the a and b axes with the interatomic distance of 2.43 Å and align linearly along the c axis with the interatomic distance of 2.58 Å. Then, the four 1st NN atomic sites from an atomic site exist along the a and b axes, the two 2nd NN atomic sites align exist along the c axis with the interatomic distance of 2.58 Å, the four 3rd NN atomic sites exist on the a-c and b-c planes with the interatomic distance of 3.04 Å, and so on. (See Fig.2, where the numbers(1∼5) indicate the (initial) 1st∼5th NN atomic sites from a Ti/Ni atom in their optimized structures.)

For comparison, we also calculate PIEs without structural optimization,$\Delta E_{\rm fix}^{\rm TM\text{-}TM}(R)$, which are defined by the same as Eq.(1) but with the fixed structure of ideal β-Sn type lattice. It is noted that a PIE with the optimized structure, $\Delta E_{\rm opt}^{\rm TM\text{-}TM}(R)$ may sometimes become higher than the corresponding PIE with the fixed structure, $\Delta E_{\rm fix}^{\rm TM\text{-}TM}(R)$ while the total energy with the optimized structure, $E_{\rm opt}^{\rm TM\text{-}TM}(R)$ is always lower than the corresponding total energy with the fixed structure, $E_{\rm fix}^{\rm TM\text{-}TM}(R)$.

To assess the accuracy of calculations with the supercell, we calculated total energies of the following base systems; the total energy of Si_{432} without Ti/Ni atom, $E_{\rm opt}^{0}$, those of $TMSi_{431}$, $E_{\rm opt}^{\rm TM}$, where a TM atom is located at the center of one of Si_{216} cuboid cells, and compared those energies with the approximated $E_{\rm opt}^{\rm TM\text{-}TM}(\infty)$ as follows:

$$\Delta A_{\rm opt}^{\rm TM\text{-}TM} = E_{\rm opt}^{\rm TM} - (E_{\rm opt}^{0} + E_{\rm opt}^{\rm TM\text{-}TM}(\infty))/2. \quad (2)$$

For Ti-Ni sytem, we take a following formula,

$$\Delta A_{\rm opt}^{\rm Ti\text{-}Ni} = (E_{\rm opt}^{\rm Ti} + E_{\rm opt}^{\rm Ni})/2 - (E_{\rm opt}^{0} + E_{\rm opt}^{\rm Ti\text{-}Ni}(\infty))/2. \quad (3)$$

The value of $\Delta A_{\rm opt}^{\rm TM\text{-}TM}$ is -0.021, -0.022 and 0.083 eV per supercell for Ti-Ti, Ti-Ni, and Ni-Ni, respectively. Then, the accuracy of the present PIE is at most 10^{-2} eV.

All the PIE calculations and structural optimizations are performed with VASP5.3, a plane-wave based density functional calculation package[13]. We employ the projector augmented-potential (PAW)[14] for the core orbitals under the generalized gradient approximation (GGA: PBE).[15])

Semi-core 3p states are treated as valence states for Ti and Ni atoms. The cutoff energy for the plane wave basis is 367.945eV (ACCURATE precision in VASP). The calculations are performed in $6 \times 3 \times 6$-unit cell of β-Sn type Si with Γ-point approximation. The structures are fully optimized by the quasi-Newton algorithm until the change in total energy is smaller than 10^{-3} eV between two steps of ionic relaxation.

3. Results and discussion

3.1. Deviations of atom positions around a substitutional Ti/Ni atom in β-Sn type Si lattice

We show the change of local structure of β-Sn type Si lattice around a substitutional single Ti/Ni atom before discussing the PIEs. Figure 1 shows deviations of the atom positions from the initial (ideal) lattice points in β-Sn type Si around (a) a Ti atom and (b) a Ni atom as a function of the optimized interatomic distance from the substitutional Ti/Ni atom. A circle indicates the averaged deviations of the n-th NN atom positions ($n = 1 \sim 12$) from the initial lattice points, where the deviation $\Delta R(\%)$ is expressed as a ratio to the Si-Si bond length ($d_{\mathrm{Si-Si}}$ =2.43 Å);

$$\Delta R = \frac{|\vec{R}_f - \vec{R}_i|}{d_{\mathrm{Si-Si}}}. \qquad (4)$$

$\vec{R}_i$ ($\vec{R}_f$) is the initial atomic position (the atomic position after the optimization). The vertical (horizontal) error bar shows the distribution of deviation (the distribution of the interatomic distance) at the equivalent n-th NN atomic sites. The vertical dashed lines indicate the initial (ideal) interatomic distances between the Ti/Ni and the n-th NN Si atoms.

As shown in Fig.1 (a), the substitutional Ti atom is displaced by about 15 % of $d_{\mathrm{Si-Si}}$. The deviation occurs along the c-axis from the initial lattice point (along the direction to one of the 2nd NN Si atom position). As a result, large deviations also appear at the 2nd and 9th NN Si positions, which align along the c-axis. However, the change of the interatomic distance between the Ti atom and the 2nd NN Si atom is not large although the deviation is larger than 10%. This is because the displacements of the 2nd NN Si atoms occur in accordance with the displacement of the Ti atom.

The interatomic distances between the Ti atom and the 1st NN Si atoms are lengthened and close to those for the 2nd NN Si atoms because of a large atomic radius and the displacement of Ti atom. For the interatomic distances between the Ti atom and the 3rd NN Si atoms, two of them on the b-c plane (on the a-c plane) are shortened (lengthened). These displacements are also due to the displacements of Ti atom and the 2nd NN Si atoms. As a result, as shown dark-colored bonds in Fig.2(a), the two 1st, the two 2nd, and the two 3rd NN Si atoms form a distorted hexagonal lattice on the b-c plane. These lattice distortions are expected to affect strongly the pair interaction energy of TM atoms in the Si lattice. It is noted that the hexagonal structure of Si atoms is commonly observed in (Ti/V/Cr)Si_2 alloy but not in (Fe/Co/Ni)Si_2 silicides.

The profile of the deviations of Si atom positions around the Ni atom in Fig.1(b) is similar to that around the Ti atom in Fig.1(a). However, the Ni atom is displaced not so much as the Ti atom. No significant structural change appears in the Si lattice around the Ni atom as shown in Fig.2(b). Figs.1(b) and 2(b) seem to indicate simple contractions of the 1st∼3rd NN Si lattice points around the Ni atom.

3.2. Pair interaction energies and local structures of Ti-Ti, Ti-Ni and Ni-Ni in β-Sn type Si

Figure 3 shows the pair interaction energies (PIEs) of (a) Ti- Ti, (b)Ti-Ni and (c) Ni-Ni pair at the substitutional sites in the β-Sn type Si as a function of interatomic distance of the two TM atoms. In the figure, vertical broken lines indicate the ideal distances between the substitutional sites. A square on the vertical broken line indicates the PIE with the fixed structure on the ideal Si lattice points. A circle indicates the PIE with the optimized structure, where all positions of impurities and Si atoms are optimized. A horizontal line arrowed to the circle of PIE shows deviation of the interatomic distance from the initial value. Vertical lines capped with symbols on the bottom of each figure indicate the interatomic distances of Ti-Ti, Ti-Ni and Ni-Ni pairs in the related Si-rich ordered silicides as references (circle for $TiSi_2$-C54(oF24), triangle for $TiSi_2$-C49(oS12), square for $Ti_4Ni_4Si_7$(tI60) and diamond for $NiSi_2$(cF12)); the height of the line indicates a number of pairs at the distance in the silicides.

Some largely negative PIEs with large structural change appear in Ti-Ti PIEs with the structural optimization in Fig.3(a); PIE of -1.1 eV at interatomic distance of about 3.1 Å(indicated by 4a), which moves from the 5th NN initial distance, and those of about -0.8 eV at about 4.7 Å(indicated by 4c), which move from the 11th and 12th NN initial distances. It is remarkable that these optimized Ti-Ti distances with the negative PIEs agree with those in Si-rich Ti alloys indicated by capped vertical lines. Thus, these negative PIEs indicate a stability of the local structures with these Ti-Ti distances. However, there also exists a positive PIE at about 3.2 Å(indicated by 4b) nearby that with the negitive PIE (3.1Å), so it is obvious that the negative PIE cannot be determined only from the interatomic distance, but depends on the local atomic structure.

Figure 4 indicates the optimized local structures, (a) with the negative PIE and (b) with the positive PIE at the similar Ti-Ti distance of 3.1-3.2 Å. As shown in Fig.4(a), two Ti atoms come closer to each other by their interaction from the initial distance of the 5th NN, and make a distorted Si-hexagon between them. Very distorted two hexagons also appear around the Ti atoms by the same manner in Fig.2(a). On the other hand, no hexagon appears and in Fig.4(b), where Ti-Ti pair enlarges the inter-

atomic distance in comparison with the that between the 3rd NN lattice points and prevents to form the Si-hexagon, which is formed if Ti atoms were sufficiently separated. The local structure around Ti-Ti pair with another largely negative PIE at Ti-Ti distance of 4.7 Åalso yields two Si-hexagons around Ti atoms as shown in Fig.4(c), as well as in Fig.2(b).

The same situation as the Ti-Ti PIEs is observed in Ti-Ni PIEs in Fig.3(b): Largely negative Ti-Ni PIEs with large structural change appear at about 2.9 and 3.6 Å. These optimized Ti-Ni distance agrees with that in ordered compound, $Ti_4Ni_4Si_7$ indicated by the capped vertical line.

Figure 5(a) shows the local structures of the Ti-Ni pair with the negative PIE at 2.9 Å. Similarly to Figs.4(a) and (c) for Ti-Ti pair, Fig.5(a) shows a Si-hexagon around the Ti atom, which seems to stabilize the local structure. There also exists a positive PIE about 2.7 Å, which is close to that of the negative PIE at 2.9 Å. No Si-hexagon appears in the local structure for the positive PIE at as shown in Fig.5(b), where the Ti-Ni pair keeps the zig-zag structure along a-axis in the β-Sn type lattice. Another negative PIE appears at around 4.4Å, which is also close to one of Ti-Ni distance in $Ti_4Ni_4Si_7$, 4.6 Å, and the local structure shown in Fig.5(c) also has a Si-hexagon.

Contrary to the PIEs of Ti-Ti and Ti-Ni, no negative PIE is found for Ni-Ni pair in Fig.3(c). Structural changes by the optimization are small, and PIEs almost monotonically decrease with increasing Ni-Ni distance. Then we find no relationship between the interatomic distances of ordered alloys and the profile of PIEs, and cannot deduce any information about local structure around Ni-Ni pairs in Si. This may be because Ni-Si interaction in Si-rich alloys is mainly sp^3-like as in the ordered $NiSi_2$, and is not reproduced by Ni-Ni pair in β-Sn type Si lattice.

Figure 6 shows Ni-Ni PIEs as the same as Fig.3(c) but in the substitutional sites in diamond Si lattice. Here, we employ a supercell of Ni_2Si_{430} ($6 \times 3 \times 3$-unit cell of diamond type Si).

First of all, we can notice that Ni-Ni interatomic distances in the Si-rich alloys shown by the capped vertical lines almost agree with the ideal interatomic distances in diamond-Si indicated by broken lines. Then, it is expected that local environment of Ni-Ni pair in Si-rich alloys, such as local atomic structure and bonding properties is similar to that in diamond-Si. The Ni-Ni PIEs are negative up the 3rd NN(4.5 Å) and Ni-Ni distances are similar to those of Si-Si in diamond Si after structural optimization. Not shown here, we have also obtained Ni-Ni PIEs at the tetrahedral interstitial sites in diamond type Si. The optimized Ni-Ni interatomic distances at the tetrahedral sites almost agree with those of Si-Si in diamond type lattice, as well as those of Ni-Ni at the substitutional sites in Fig.6.

Therefore, we conclude that the optimized structures around Ti-Ti and Ti-Ni pairs with negative PIEs in β-Sn type Si give significant information about local structures of not only ordered but also disordered or amorphous Si-rich Ti and Ti-Ni alloys while structures around Ni-Ni pairs in Si-rich alloys are mainly governed by sp^3-like Si-bonds.

4. Conclusions

To discuss local environments and to find typical local structures of transition-metal (TM) atoms in Si-rich amorphous silicides or alloys, we calculate pair interaction energies (PIEs) of Ti-Ti, Ti-Ni and Ni-Ni pairs and optimized local structures around the pairs in β-Sn type Si by first principles calculation. We found from interatomic distance dependences of PIEs up to the 12th nearest NN that interatomic distances of Ti-Ti and Ti-Ni pairs with largely negative PIEs agree with those in Si-rich ordered silicides such as $TiSi_2$ and $Ti_4Ni_4Si_7$, and that the optimized local structures around Ti-Ti and Ti-Ni pairs have Si-hexagons, which are typically shown in early-TM silicides, and expected to be observed in the amorphous Si-rich silicides or alloys. On the contrary, Ni-Ni pair in β-Sn type Si indicates no significant feature in PIE profile or in local structures.

Acknowledgement

Authors are grateful for the financial support from the Ministry of the Education, Culture, Science and Technology of Japan(JSPS KAKENHI Grand No.15K06422).

References

[1] E. Ma, Growth of amorphous silicide during Ti/Si interfacial reactions in multilayer thin films, Mater. Sci. Eng.: A 398 (2005) 60–65. doi:10.1016/j.msea.2005.02.059.

[2] N. Okada, N. Uchida, T. Kanayama, Low-barrier heterojunction of epitaxial silicide composed of W-encapsulating Si clusters with n-type Si, Appl. Phys. Lett. 101 (2012) 212103. doi:10.1063/1.4767136.

[3] N. Okada, N. Uchida, T. Kanayama, Thermal stability of amorphous Si-rich W silicide films composed of W-atom-encapsulated Si clusters, J. Appl. Phys. 121 (2017) 225308. doi:10.1063/1.4985248.

[4] N. Uchida, T. Miyazaki, Y. Matsushita, K. Sameshima, T. Kanayama, New semiconducting silicides assembled from transition-metal-encapsulating Si clusters, Thin Solid Films 519 (2011) 8456–8460. doi:10.1016/j.tsf.2011.05.019.

[5] M. Fukuhara, K. Sugawara, Electric charging/discharging characteristics of super capacitor, using de-alloying and anodic oxidized Ti-Ni-Si amorphous alloy ribbons, Nanoscale Res. Lett. 9 (2014) 253. doi:10.1186/1556-276X-9-253.

[6] M. Fukuhara, T. Kuroda, F. Hasegawa, Amorphous titanium-oxide supercapacitors, Sci. Rep. 6 (2016) 35870. doi:10.1038/srep35870.

[7] T. A. Yersak, S. B. Son, J. S. Cho, S. S. Suh, Y. U. Kim, J. T. Moon, K. H. Oh, S. H. Lee, An all-solid-State Li-ion battery with a pre-lithiated Si-Ti-Ni alloy anode, J. Electrochem. Soc. 160 (2013) A1497–A1501. doi:10.1149/2.086309jes.

[8] Z. Z. Zhang, B. Partoens, K. Chang, F. M. Peeters, First-principles study of transition metal impurities in Si, Phys. Rev. B 77 (2008) 155201. doi:10.1103/PhysRevB.77.155201.

[9] Y. Kamon, H. Harima, A. Yanase, H. Katayama-Yoshida, Ultrafast diffusion mechanism of the late 3d transition metal impuritties in silicon, Physica B 308–310 (2001) 391–395. doi:10.1016/S0921-4526(01)00754-2.

[10] T. Hoshino, N. Fujima, M. Asato, R. Tamura, Medium-ranged interactions of transition-metal (3d and 4d) inpurity pairs in Al and atomic structures of Al-rich Al-transition-metal alloys , J. Alloy. Comp. 434-435 (2007) 572–576. doi:10.1016/j.jallcom.2006.08.191.

[11] T. Hoshino, M. Asato, S. Tanaka, F. Nakamura, N. Fujima, First-principles calculations for stability of atomic structures of Al-rich AlX (X=Sc-Zn) alloys, including AlMn quasicrystal: II. Medium-ranged interactions of X pairs in Al, Intermetallics 14 (2006) 913–916. doi:10.1016/j.intermet.2006.01.009.

[12] T. Hasegawa, K. Osaka, T. Takama, H. Chen, Short-range order structure and effective pair-interaction energy in NiSi alloys, Acta Mater. 55 (2007) 5382–5388. doi:10.1016/j.actamat.2007.05.053.

[13] G. Kresse, J. Furthmüller, Efficient iterative schemes for ab initio total-energy calculations using a plane-wave basis set, Phys. Rev. B 54 (1996) 11169. doi:10.1103/PhysRevB.54.11169.

[14] G. Kresse, D. Joubert, From ultrasoft pseudopotentials to the projector augmented-wave method, Phys. Rev. B 59 (1999) 1758–1775. doi:10.1103/PhysRevB.59.1758.

[15] J. P. Perdew, A. Ruzsinszky, G. Csonka, O. A. Vydrov, G. E. Scuseria, L. A. Constantin, X. Zhou, K. Burke, Restoring the density-gradient expansion for exchange in solids and surfaces, Phys. Rev. Lett. 100 (2008) 136406. doi:10.1103/PhysRevLett.100.136406.

Figure captions

Figure 1. Deviations of atom positions from the initial(ideal) lattice points around a substitutional Ti and Ni atom in β-Sn type Si as a function of the optimized interatomic distances between Ti/Ni and Si atoms. The deviation is expressed as a ratio to the 1st NN Si bond length (2.43 Å). The vertical (horizontal) error bar shows the distribution of deviation (interatomic distance) around the value (circle) averaged on the equivalent lattice points. The vertical dashed lines indicate the initial(ideal) interatomic distances.

Figure 2. Local atomic structures of β-Sn type Si around (a) Ti and (b) Ni atoms. The Si lattice is largely distored around a Ti atom, and constitutes a distorted hexagon (indicated by dark-colored bonds of 2.45-2.79 Å). The numbers (1∼5) indicate the initial atomic sites of the n-th ($n = 1 \sim 5$) NN Si atoms from Ti/Ni atoms.

Figure 3. Pair interaction energies of (a) Ti-Ti, (b) Ti-Ni and (c) Ni-Ni at the substitutional sites in the β-Sn type Si as a function of interatomic distance of the two TM atoms. Vertical broken lines indicate the ideal distances between the substitutional sites. A square on the vertical broken line indicates the PIE with the fixed structure on the ideal (initial) Si lattice. A circle indicates the PIE with the optimized structure. A horizontal line arrowed to the circle of PIE shows deviation of the interatomic distance from the initial value. Vertical lines capped with symbols indicate the interatomic distances of Ti-Ti, Ti-Ni and Ni-Ni pairs in the related Si-rich ordered silicides.

Figure 4. Local atomic structures of β-Sn type Si around (a) the 5th NN Ti-Ti pair, (b) the 3rd NN Ti-Ti pair, which have a similar interatomic distance of 3.1-3.2 Å, but have oppositly different PIEs (-1.1 eV(4a) and +0.3 eV(4b) in Fig.3(a)), and (c) the 12th NN Ti-Ti- pair with PIE of -0.8 eV(4c).

Figure 5. Local atomic structures of β-Sn type Si around (a) the 4th NN Ti-Ni pair, (b) the 2nd NN Ti-Ni pair, which have a similar interatomic distance of 2.7-2.9 Å, but have oppositly different PIEs(-0.7 eV(5a) and +0.8 eV(5b) in Fig.3(b)), and (c) the 6th NN Ti-Ti- pair with PIE of -0.6 eV(5c). .

Figure 6. The same as Fig.3(c) for Ni-Ni at substitutional sites in the diamond type Si.

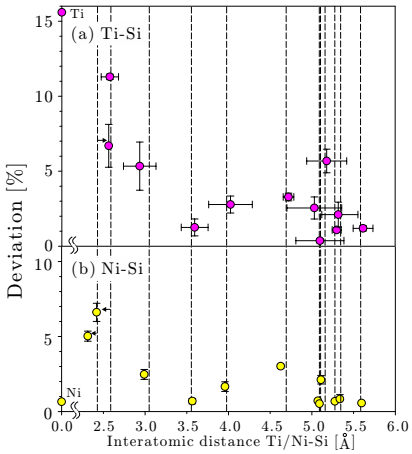

Figure 1: Deviations of atom positions from the initial(ideal) lattice points around a substitutional Ti and Ni atom in β-Sn type Si as a function of the optimized interatomic distances between Ti/Ni and Si atoms. The deviation is expressed as a ratio to the 1st NN Si bond length (2.432 Å). The vertical (horizontal) error bar shows the distribution of deviation (interatomic distance) around the value (circle) averaged on the equivalent lattice points. The vertical dashed lines indicate the initial(ideal) interatomic distances.

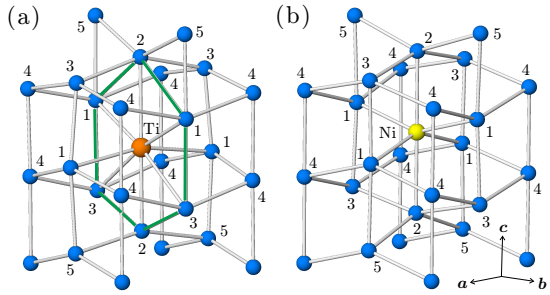

Figure 2: Local atomic structures of β-Sn type Si around (a) Ti and (b) Ni atoms. The Si lattice is largely distored around a Ti atom, and constitutes a distorted hexagon (indicated by dark-colored bonds of 2.45-2.79 Å). The numbers (1∼5) indicate the initial atomic sites of the n-th ($n = 1 \sim 5$) NN Si atoms from Ti/Ni atoms.

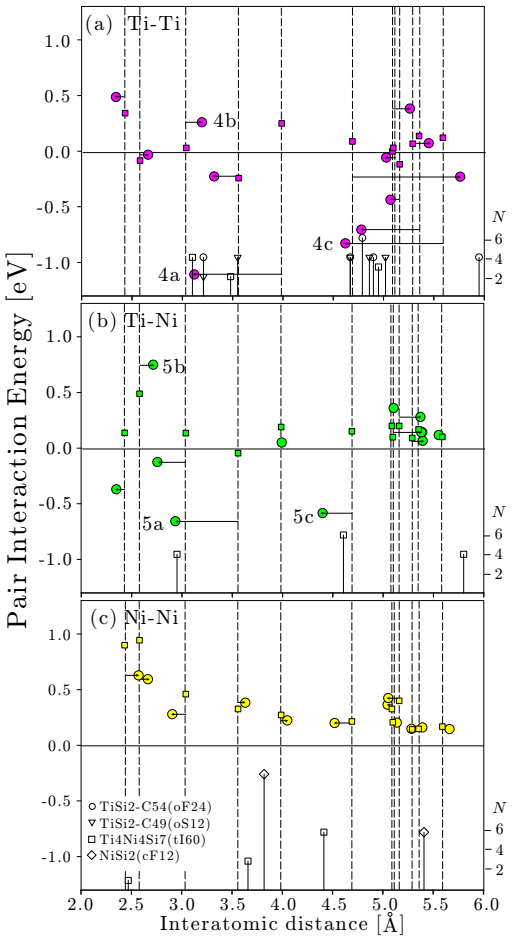

Figure 3: Pair interaction energies of (a) Ti-Ti, (b) Ti-Ni and (c) Ni-Ni at the substitutional sites in the β-Sn type Si as a function of interatomic distance of the two TM atoms. Vertical broken lines indicate the ideal distances between the substitutional sites. A square on the vertical broken line indicates the PIE with the fixed structure on the ideal (initial) Si lattice. A circle indicates the PIE with the optimized structure. A horizontal line arrowed to the circle of PIE shows deviation of the interatomic distance from the initial value. Vertical lines capped with symbols indicate the interatomic distances of Ti-Ti, Ti-Ni and Ni-Ni pairs in the related Si-rich ordered silicides.

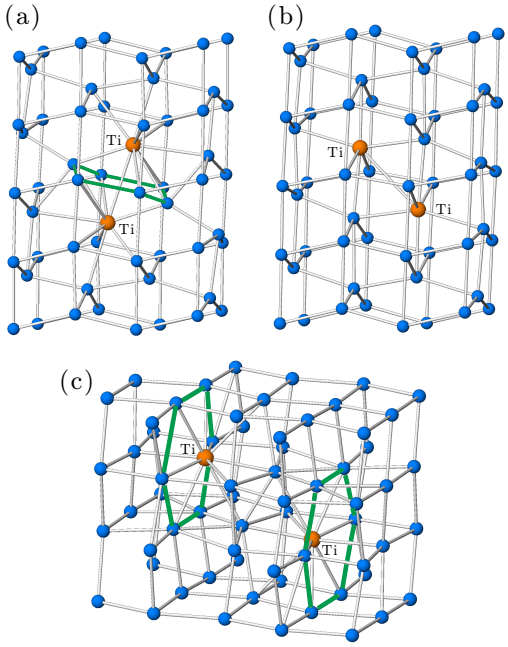

Figure 4: Local atomic structures of β-Sn type Si around (a) the 5th NN Ti-Ti pair, (b) the 3rd NN Ti-Ti pair, which have a similar interatomic distance of 3.1-3.2 Å, but have oppositly different PIEs (-1.1 eV(4a) and +0.3 eV(4b) in Fig.3(a)), and (c) the 12th NN Ti-Ti-pair with PIE of -0.8 eV(4c).

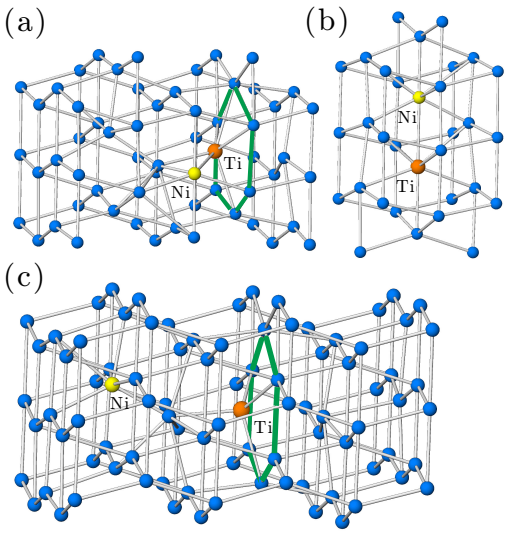

Figure 5: Local atomic structures of β-Sn type Si around (a) the 4th NN Ti-Ni pair, (b) the 2nd NN Ti-Ni pair, which have a similar interatomic distance of 2.7-2.9 Å, but have oppositly different PIEs(-0.7 eV(5a) and +0.8 eV(5b) in Fig.3(b)), and (c) the 6th NN Ti-Ti-pair with PIE of -0.6 eV(5c). .

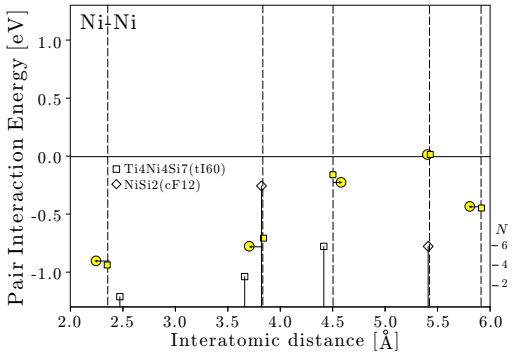

Figure 6: The same as Fig.3(c) for Ni-Ni at substitutional sites in the diamond type Si.